

Investigation of Silver Recovery from Thin Film CIGS Solar Cells by Selective Leaching

A Statistic Approach

Master's thesis in Material's Chemistry

Rasmus Fransson

MASTER'S THESIS

Investigation of Silver Recovery from Thin Film CIGS Solar Cells by Selective Leaching

A Statistic Approach

Rasmus Fransson



CHALMERS
UNIVERSITY OF TECHNOLOGY

Department of Chemistry and Chemical Engineering
Industrial Materials Recycling
CHALMERS UNIVERSITY OF TECHNOLOGY
Gothenburg, Sweden 2020

Investigation of Silver Recovery from Thin Film CIGS Solar Cells by Selective Leaching
A Statistic Approach
Rasmus Fransson

© Rasmus Fransson, 2020.

Supervisor: Burçak Ebin, Industrial Materials Recycling
Examiner: Martina Petranikova, Industrial Materials Recycling

Master's Thesis
Department of Chemistry and Chemical Engineering
Industrial Materials Recycling
Chalmers University of Technology
SE-412 96 Gothenburg
Telephone +46 31 772 1000

Cover: Response surface of silver purity by time as a function of time and acid concentration found at the end of the results section.

Typeset in L^AT_EX
Printed by Chalmers Reproservice
Gothenburg, Sweden 2020

Investigation of Silver Recovery from Thin Film CIGS Solar Cells by Selective Leaching

A Statistic Approach

Rasmus Fransson

Department of Chemistry and Chemical Engineering

Chalmers University of Technology

Abstract

Recycling and green energy has become increasingly hot topics in research and our everyday lives. One of the promising sources of green energy that is being developed is CIGS thin film solar cells, the photovoltaic cell contains an alloy of copper, indium, gallium and selenium where silver is used as a conducting material on the surface. However, innovative and sustainable strategies to recover silver from spent CIGS solar cells are still not readily available. Previous research has shown strategies including pyrolysis and electrodeposition, both which are energy consuming and require multiple steps prior to the separation stage. Reducing the number of pre-treatment steps will play an important role in realizing sustainable silver recovery. This study aims to investigate selective leaching as a feasible method of recovering metals, especially silver, from CIGS solar cells. This was achieved by combining thermodynamic investigation, analyzing old data combined with new leaching experiments to design a statistical model. A second aim is to evaluate different factors and their contribution to dissolution of silver. A model describing the system as a function of time, acid concentration and solid to liquid ratio was made using Design of Experiments (DOE) and Analysis of Variance (ANOVA). It was shown that silver can be selectively leached by nitric acid with a resulting purity above 90 % after 1 h. The results show that the significant factors are time and nitric acid concentration. The major co-dissolved metal component is indium but low levels of tin is also found in the leachate. In the initial experiments of the study it was found that oxalic acid leaching may be an alternative route for simultaneous silver and indium recovery due to silver being precipitated while indium is found in the leachate, but further research should be conducted.

Keywords: Silver, selective leaching, CIGS, recycling, solar cells, nitric acid, organic acids, factorial design, statistical modelling.

Acknowledgements

First and foremost I want to thank Burçak Ebin for very valuable guidance and discussions during my stay here at IMR. Second I want to thank Martina Petranikova for being my examiner and Jonas Schuster for support in ICP-MS handling and help in the lab. Third I want to thank Midsummer AB for providing sample solar cells for me to test. Last but not least I want to thank all of you working at NC and IMR here at Chalmers for having me, everyone has been really friendly and helpful in times of need.

Rasmus Fransson, Gothenburg, June 2020

Contents

List of Acronyms	xi
List of Figures	xiii
List of Tables	xv
1 Introduction	1
1.1 CIGS Solar Cells	2
2 Theory	5
2.1 Thermodynamic Investigation by Calculations	5
2.2 Leaching	6
2.2.1 Design of Experiments	6
2.3 Analysis Instruments	8
2.3.1 Inductively Coupled Plasma - Mass Spectrometer	8
2.3.2 Scanning Electron Microscope	9
3 Methods	11
3.1 Thermodynamic Investigation	11
3.2 Preparation of Solar Cell Samples	12
3.3 Vaporisation Test	12
3.4 Leaching Experiments	13
3.5 Sample Analysis	13
3.6 Factorial Design	13
4 Results and Discussion	15
4.1 Thermodynamic Investigation	15
4.2 Vaporization Test	17
4.3 Initial Leaching Experiments	18
4.4 Design of experiments	21
5 Conclusions	25
Bibliography	27
A Appendix 1 - Design of Experiments Data	I
B Appendix 2 - SEM and EDS images	III

C Supplementary Data

VII

Acronyms

Symbols

ΔG Gibbs free energy

ΔG° Gibbs standard free energy

μ Average

σ Standard Deviation

σ^2 Variance

A

ANOVA Analysis of Variance

C

c-Si Crystalline Silicon

CIGS Copper Indium Gallium Selenide

CIS CuInSe_2

D

DOE Design of Experiments

E

EDX Energy-dispersive X-ray spectroscopy

EU European Union

I

ICP-MS Inductively Coupled Plasma - Mass Spectrometer

IRENA International Renewable Energy Agency

ITO Indium Tin Oxide

P

ppm Parts Per Million

PV Photovoltaic

S

SEM Scanning Electron Microscope

U

UN United Nations

List of Figures

1.1	Statistics on the photo-voltaic solar cell capacity of Europe and China from 2009 to 2018 [3].	2
1.2	a) Tetragonal chalcopyrite crystal structure, the CIGS unit cell b) Schematic overview of a CIGS solar cell. [12].	3
1.3	Pie chart diagram of solar cell market share in 2014 by Jeyakumar Ramanujam et al. [6]	4
2.1	A geometrical illustration of a 2^3 factorial design.	7
2.2	A schematic overview of an ICP torch with inlets, and plasma.	9
3.1	Three different solar cell samples cut into 3×5 cm ² rectangles with the large silver line centered.	12
4.1	ΔG° for the dissolution of silver with different organic acids.	15
4.2	ΔG° for reactions with CIGS elements with citric acid.	16
4.3	ΔG° for ITO reaction with nitric acid and oxalic acid.	16
4.4	Logarithmic value of reaction equilibrium constant for ITO reaction with nitric acid and oxalic acid.	17
4.5	Concentrations of metals during leaching with nitric acid, maleic acid, oxalic acid and citric acid.	18
4.6	SEM images of a sample after 24 h oxalic acid leaching (left) and a fresh sample (right).	19
4.7	EDS analysis on silver conducting line after 24 h oxalic acid leaching.	19
4.8	XRD spectrum of the residue of the oxalic acid leaching.	20
4.9	Response surface for silver purity model as a function of time (x) vs acid concentration (y) with silver purity % response (z). Brighter color is higher purity.	23
4.10	The response surface for silver purity divided by time, take note that it has the same shape as figure 4.9 but inverted. X represents time, Y represents acid concentration and Z is the purity divided by time.	24
B.1	Analysis of fresh solar cell showing original composition of silver line.	IV
B.2	Analysis of cell after 24 h of oxalic acid leaching on silver line. No Silver present. Bottom image is EDX of the black lump.	V
C.1	An image taken above the beaker of the oxalic acid leaching sample after 4 h and 24 h respectively. Notice the slight purple tint of the otherwise green cell and that the leachate had turned purple after 24 h.	VIII

List of Tables

2.1	The identity matrix for a 2^3 factorial design.	7
3.1	Acids used for leaching, their purity and at what concentrations they were used.	13
4.1	The volumes before and after 24 hours in the three beakers with and without cover at maximum airflow.	17
4.2	The design of experiments with result values from Steenari et al. [14] and initial experiments done in this research. The sign table represents the level of the parameter value, a plus sign '+' represents the high value and a minus sign '-' represents the low value of the parameters where A = time, B = Acid concentration and C = S/L ratio. There are two result columns, one for each repetition.	21
4.3	The relative silver purity, total silver concentration divided by total metal concentration per sample.	22
4.4	Effect estimate summary for maximum silver purity. Percent contribution relates to model effect contribution.	22
4.5	ANOVA table for silver purity model, a P-value below 0.05 is considered significant.	22
A.1	Summary of effects when optimizing towards maximum silver concentration.	I
A.2	ANOVA table for maximum silver concentration after investigating each leaching parameter in the factorial experiment.	I
A.3	predicted model for maximum silver concentration.	II
A.4	ANOVA table for Silver purity per hour.	II

1

Introduction

Global goals in renewable energy includes improvements and expansion of solar power as a type of clean energy. Included in United Nations (UN)'s sustainable development goals, point 7 “affordable and clean energy”, the following statements are made:

- **7.1** By 2030, ensure universal access to affordable, reliable and modern energy services
- **7.2** By 2030, increase substantially the share of renewable energy in the global energy mix
- **7.3** By 2030, double the global rate of improvement in energy efficiency

In addition to these statements there are points describing accessibility to research and clean energy sources [1]. Solar power is one of many alternatives to fossil fuels as stated earlier, different types of Photovoltaic (PV) cells are being developed and improved by researchers all around the world. Research and development in addition to solar module market conditions has lead to a solar module prize decrease of 75 % the last ten years [2]. Since solar power capacity is being expanded both in the private sector and by countries, the amount of solar cell waste will increase accordingly [3].

The solar cell production is dominated by China with focus on expanding their solar cell capacity and electricity production. This makes China the world leading nation in solar cell capacity as can be seen in fig 1.1 [4]. However, the expansion is yet to reach its peak with high expectations on solar energy to become the “energy of the future”. International Renewable Energy Agency (IRENA), published a report on end of life management of solar panels which included a global projection on the solar power capacity in 10 respectively in 30 years. It shows that the top 3 contributors to solar panel waste will accumulate between 1.7 to 8 million metric tonnes of waste in ten years in comparison to 40 000-250 000 tonnes of waste accumulated until 2014. Regarding waste management regulations, European Union (EU) is alone to have adopted specific PV-cell regulations [5]. With an underdeveloped recycling program, as accumulating waste suggests, it is safe to say that feasible recycling strategies with high yields will play an important role in the near future.

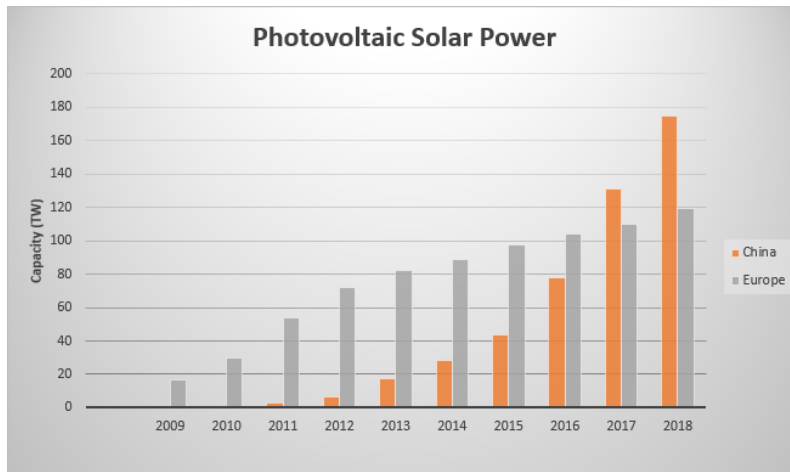


Figure 1.1: Statistics on the photo-voltaic solar cell capacity of Europe and China from 2009 to 2018 [3].

There are different solar cells available on the market today, all of which need focus in recycling research. The main types of solar cells on the market today are single- and poly crystalline silicon cells, cadmium tellurium and CIGS solar cells [6]. In this study one type of cell is investigated, the inorganic CIGS type solar cell.

1.1 CIGS Solar Cells

Initially CuInSe_2 (CIS) was discovered and was first synthesised 1956. The material showed promising photovoltaic properties and was further developed by adding gallium. This novel structure is currently being developed as a type of thin film solar cells, Copper Indium Gallium Selenide (CIGS) [7]. The valence structure of the CIGS material belongs to the II-III-IV₂ family, where the roman numbers signify number of valence electrons of the elements. This results in a chemical composition of $\text{CuIn}_{1-x}\text{Ga}_x\text{Se}_2$, which forms a crystal structure that can be described as tetragonal chalcopyrite which can be seen in fig 1.2a. [8] By gradually changing the gallium ratio throughout the cell a more efficient light absorption can be achieved by increasing the CIGS bandgap from 1.04 eV to 1.7 eV when all indium is replaced [9]. By adding a cadmium sulphide layer the efficiency of the solar cell could be increased even further by absorbing photons with energies above 2.4 eV [10]. Since cadmium is both rare and toxic, it has been abandoned and replaced with either a zinc tin oxide (ZnSnO) layer or Indium Tin Oxide (ITO) layer. On top of the CIGS layer are conducting lines of silver to deliver the produced electricity. The CIGS investigated in this study use ITO and a schematic overview can be seen in 1.2b [11].

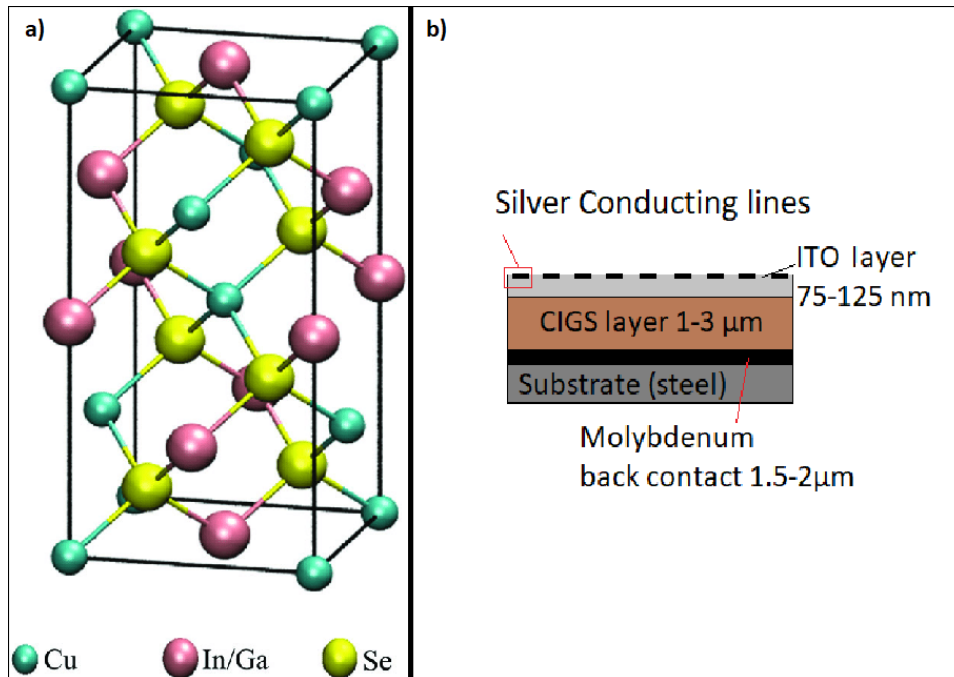


Figure 1.2: a) Tetragonal chalcopyrite crystal structure, the CIGS unit cell b) Schematic overview of a CIGS solar cell. [12].

The greatest benefit with CIGS is that the absorbing layer can be made very thin and therefore more resistant to physical damage with the potential to absorb more light than c-Si solar cells by adding several layers [10].

Since the main scope of this study is to separate the silver from the CIGS solar cells, some background to why this is important is necessary. Aside from silver being a noble metal and therefore valuable, there are some other aspects to recycling it.

Silver is mainly found together with other metals such as gold, lead (in galena ore) and sulfur (in argentite ore). It is uncommon to find pure silver deposits, but they exist as well. A natural limitation to the use of silver is its rarity, in 2014 all known sources of silver added up to 540 000 tonnes. This can be compared to the global silver demand of roughly 24 000 tonnes in 2011 [13]. Around 75 % of the silver demanded comes from mines. One of the main issues with mining is that it is rough on nature, destroying the area around the excavation site. This can easily be avoided by recycling the already mined silver. The lack of feasible methods to recycle silver from spent solar cells is the main issue that needs to be addressed. That said, the solar cell industry is demanding less than 5 % of the annual silver demand in comparison to other industries such as jewellery which stands for roughly 20 %. However, jewellery can be reformed, spent solar panels and electronics contain other metals at high purity as well which makes silver recovery more demanding [13].

Previous work [14] on silver recovery from CIGS has been reported. This report is thoroughly studying nitric acid leaching as the silver dissolution step followed by either solvent extraction and electrowinning for the recovery step. Silver was successfully dissolved by using nitric acid and serves as valuable background information to this study. The vast majority of reports found are focusing on silver recovery from other sources than CIGS [15] [16] [17].

Observations of the solar panel market in 2014 show that the Crystalline Silicon (c-Si) type solar cells were the most common, as can be seen in fig 1.3. Thin film solar cells are one of the smallest fractions on the market in 2014, it is increasing but is still only a small part of the total solar cell market [18].

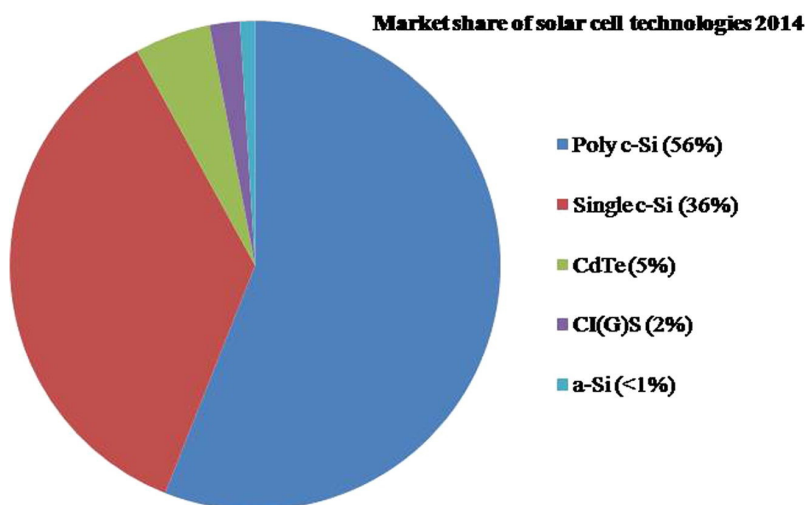


Figure 1.3: Pie chart diagram of solar cell market share in 2014 by Jeyakumar Ramanujam et al. [6]

Other novel methods using glucose for dissolution of pure silver where a two-step complex formation of silver was presented. However, only a few Parts Per Million (ppm) of silver was found in the leachate when leaching of a thin silver foil [19]. Focused on purification of silver, a study using hydrogen peroxide to purify silver containing waste, AgCl, was reported in 2017 with purity reaching 99.99% [20]. This could be a potential step to recover high purity silver crystals from the CIGS leachate.

2

Theory

2.1 Thermodynamic Investigation by Calculations

To reduce the amount of unnecessary experiments, the initial part of the study consisted of a thermodynamic investigation. It is possible to calculate whether a reaction is favored by thermodynamics by investigating the reaction's equilibrium constant (K_{eq}) and Gibbs free energy (ΔG).

The following section regarding thermodynamic equations is based on [21]. Gibbs free energy can be describes as the most amount of non-expansive work the system can produce without changing the system in regard to energy and matter. An equation describing this can be seen in 2.1.

$$\Delta G = \Delta H - T\Delta S \quad (2.1)$$

Where ΔH is enthalpy change and ΔS is entropy change of the observed system. To relate this to reactions it is possible to relate equation 2.1 to the equilibrium constant of a reaction.

$$\Delta G = \Delta G^\circ + RT\ln Q_r \quad (2.2)$$

Where ΔG° is the Gibbs free energy per mole at STP (298 K and 100 kPa) and Q_r is the reaction quotient which describes the relative concentration of reactants and products. To find ΔG for a system at equilibrium one can rewrite equation 2.2 to consider the equilibrium constant (K_{eq}) of the reaction.

$$\Delta G^\circ = -RT\ln(K_{eq}) \quad (2.3)$$

In practice a negative ΔG value means that the reaction is favored at the current conditions. However, it does not provide insight in the kinetics of the reaction and it can therefore even though favored by thermodynamics be a very slow reaction. On the other hand, positive ΔG suggests that the reaction at the investigated conditions will be at disadvantage from a thermodynamic perspective. This disadvantage may lead to another product being formed kinetically or no product being formed at all. A software, HSC Chemistry 10, by Outotec, with a database containing enthalpy, entropy and gibbs free energy data for different compounds was used for these calculations. The database consist of empirical data. It is possible to add custom data as well making it very versatile.

2.2 Leaching

Leaching is one separation method often used in hydrometallurgy. It is based on solid to liquid separation where the desired substance is solved into the leachate and thus either purifying the solid phase or recovering the substance leached. The leachate can be anything favoring the dissolution of the desired substance, it is usually dissolved in a solvent, as in this case where an acid is dissolved in water. The leaching rate is dependant on many factors, among them are diffusion rate, leachate saturation, particle size, packing of the target and the target becoming more porous as more is leached out. In addition to factors dependant on leaching time, the solid to liquid ratio, temperature and viscosity of the leachate affect leaching. Solid to liquid ratio (s/l) refers to the ratio between the sample mass and leachate volume. A higher ratio means more sample per volume leachate, for example, if the sample mass is 0.5 g and the leachate volume is 40 mL the ratio would be 1:80 g/mL and is written 1/80 [22].

In this case the desired substance is silver and is situated on the surface of the material leached from, therefore the leaching is happening on both the surface and inside the silver material. As time progress the material will become more porous as leachate penetrates the surface and thus the total surface area of silver should increase resulting in an increased leach rate. When even more silver is leached the total area will decrease until all silver has been dissolved or leachate is saturated. Other metals in the system may affect the leach rate by consuming the reactant.

2.2.1 Design of Experiments

Finding a model which describes a desired result mathematically is one of the many purposes of using Design of Experiments (DOE). Performing experiments by changing one factor at a time is time consuming and require lots of experiments and it fail to consider any interactions between factors. If many factors are changed simultaneously interactions can be found and a lot less experiments are necessary but the result analysis is different. This mindset is called design of experiments and the experiment method is called factorial design. It's fundamental concept is to find as much information as possible with as few experiments as possible while having control over the loss of data [23].

Robust design is one example of DOE, Taguchi's work describes a methodology in which the purpose is to find the most stable conditions for a process. It can be described as finding a system where the Average (μ) is at the desired level while keeping the Variance (σ^2) and thus also the Standard Deviation (σ) as small as possible. Factorial design is one of the methods to find a robust system with the least amount of experiments. By proceeding with an Analysis of Variance (ANOVA) and regression analysis of a factorial design, the reliability of the process and what factors are significant can be found [24].

For a factorial design where three parameters are investigated at two levels respectively the least amount of experiments required for finding their individual effects is 2^3 . The “2” describes the levels and “3” the number of parameters. This can be clarified with geometry, when the three parameters are varied between a high and a low value, every experiment will represent a corner point of a cube in a coordinate system where every parameter is represented by one of the axis, see figure 2.1. It is possible to find whether the effects of the parameters are linear by adding a center point. If the effects are linear the model response will form lines that pass through the center. High and low values are represented by a ‘+’ or ‘-’ in an identity matrix which can be seen in table 2.1. The corresponding high- and low values are determined by the user, they need to be greater than the resolution of the analysis method, a good rule of thumb is that the distance between them should be five times greater than the σ [25].

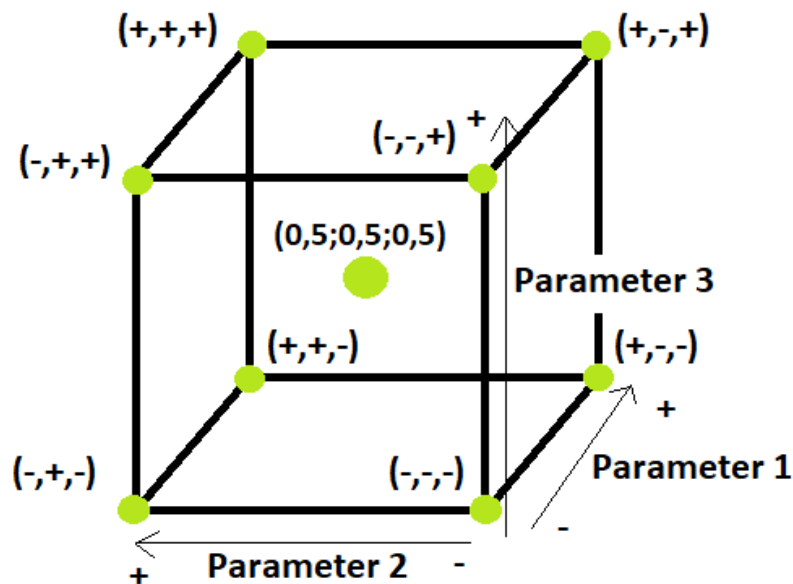


Figure 2.1: A geometrical illustration of a 2^3 factorial design.

Table 2.1: The identity matrix for a 2^3 factorial design.

A	B	C
-	-	-
+	-	-
-	+	-
+	+	-
-	-	+
+	-	+
-	+	+
+	+	+

The resulting equation describing the system, often referred to as transfer function, depends on the leaching conditions within the boundaries of the experiments and is described with terms determined by their corresponding parameters significance, in other words, how much they affect the response. In the model, β_{0-123} represents each parameter's effect, x_{1-3} represent the set value of the effect from -1 to 1 and a is the number of repetitions. An example of such a model can be seen in equation 2.4 [25].

$$y = \beta_0 + \frac{1}{a}(\beta_1x_1 + \beta_2x_2 + \beta_{23}x_2x_3 + \beta_{123}x_1x_2x_3) \quad (2.4)$$

2.3 Analysis Instruments

The analysis methods used in this study was inductively Coupled plasma mass spectrometry, electron microscopy and x-ray powder diffraction. Their basic principles will be covered in this section in order of appearance.

2.3.1 Inductively Coupled Plasma - Mass Spectrometer

Inductively Coupled Plasma - Mass Spectrometer (ICP-MS) is an analytical instrument mainly used for qualification and quantification of trace-elements. It is a combination of a sample preparation and a sample analyzing instrument.

The plasma part consists of three tubes with different functions. One connected to an ion source, usually argon gas, which is continuously ionized inside a coil at the end of the tubes which provides a strong magnetic field to stabilize and contain the plasma. The second and outermost tube serves to maintain the plasma and tubing at the right temperature, commonly referred to as the cooling gas tube. In the middle tube, the argon flow rate is lower, this is the ion source. The final and center tube is where the sample is introduced, the carrier gas is also argon. At the end of the plasma lies the entrance to the analysis instrument where the ions flow into, in this case a mass spectrometer, see fig 2.2 [26].

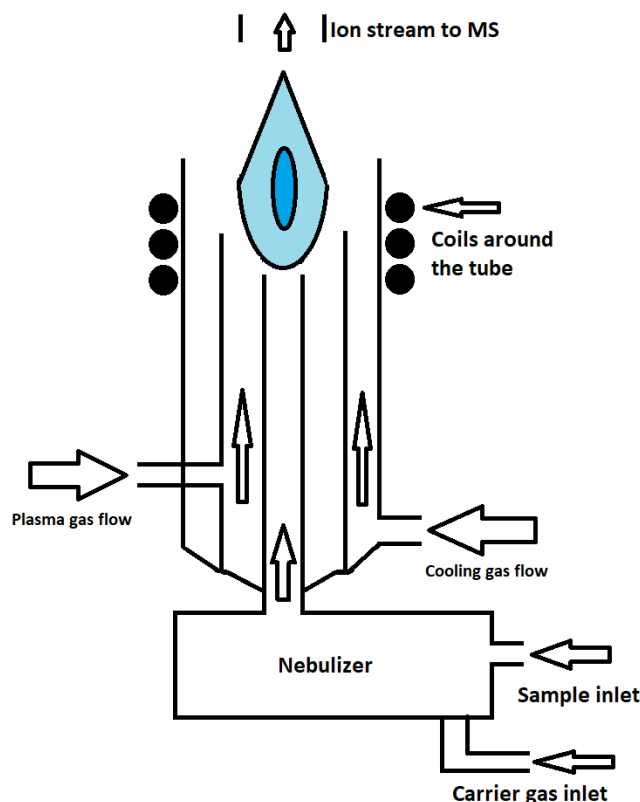


Figure 2.2: A schematic overview of an ICP torch with inlets, and plasma.

A mass spectrometer (MS) is a versatile analysis instrument and depending on the separation and ionization method it can be used to detect very low concentrations of almost any substance or metal. This was a breakthrough in analytical chemistry since it was very difficult and time consuming prior to the MS to measure different isotopes and trace amounts of elements in a sample. After a century of research and improving the instrument now days the MS is an essential tool in many fields such as nuclear chemistry, medicine for detection of drugs in blood and environmental investigations, too many different substances may make MS difficult due to interference issues however [27] [28].

The mass spectrometer consist of essentially two parts, one that ionizes the entering sample and the mass selection part. In the case of ICP-MS the plasma of the ICP ionizes the sample, the ions then enter a magnetic field which separates the sample by mass to charge ratio m/z . As the magnetic field's frequency is altered different ions will reach the detector which yield a signal interpreted by a software. The intensity of the signal is proportional to the amount of ions reaching the detector [28].

2.3.2 Scanning Electron Microscope

Imagine a light microscope, but instead of using photons to form an image you use electrons. This is exactly what a Scanning Electron Microscope (SEM) does. By using an electron gun producing electrons with an energy between 0.1-30 keV and

fixating the electron beam with electron lenses it is possible to achieve resolutions near 10 nm. Instead of the detector being your eyes it is a electron detector and by using a control console capable of interpreting the signal it allows in depth analysis of the surface of a sample [29]. In addition to high resolution imaging it is possible to run an elemental analysis of the surface of a sample with a SEM. This mode is called Energy-dispersive X-ray spectroscopy (EDX). The difference being that instead of collecting the reflected electrons from the surface, the x-rays coming from the atoms excited by the electron beam is collected and analyzed. Since every element has a unique x-ray spectrum it is possible to differentiate between them, by further investigating the intensity of the x-rays it is possible to acquire the elemental composition [30].

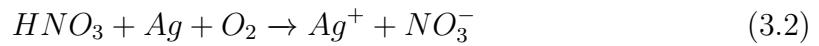
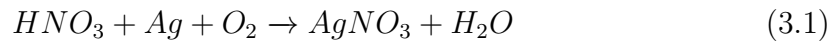
3

Methods

3.1 Thermodynamic Investigation

Potential leaching reactions with nitric, oxalic, citric, maleic, adipic and valeric acid to leach silver, ITO and CIGS respectively, were entered in the program. The results were then compared in aspect to Gibbs standard free energy (ΔG°) energy at dissolution of silver, the CIGS metals or In_2O_3 to represent ITO. If ΔG° was close to or above 0 it was abandoned. Different oxidizers were also compared. This was done by comparing silver dissolution by forming silver nitrate with H_2O_2 , NO_2 , N_2O_4 and O_2 .

The reactions were constructed as can be seen in example equation 3.1, where the salt was used as product if the data was available, otherwise the products were written as ions as seen in equation 3.2.



3.2 Preparation of Solar Cell Samples

The CIGS solar cells provided by Midsummer AB were shaped as squares with rounded corners. To reduce waste cell material the cells were cut using stationary plate shears in $3 \times 5 \text{ cm}^2$ rectangles as uniform as possible, see figure 3.1. The solar cells were cut upside down to reduce cut roughness. Every solar cell yielded 11 uniform samples.

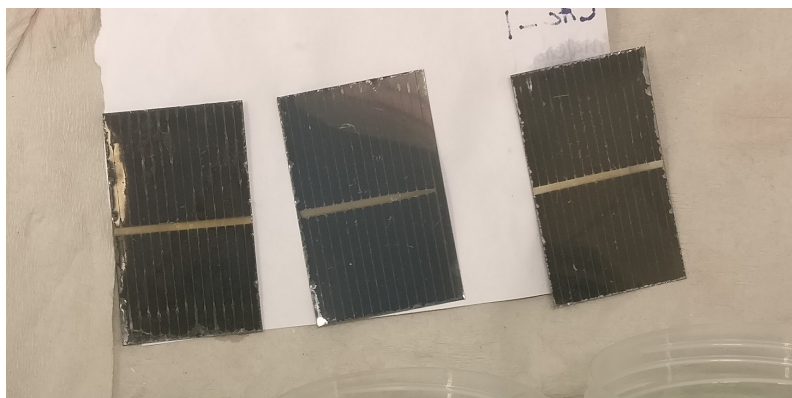


Figure 3.1: Three different solar cell samples cut into $3 \times 5 \text{ cm}^2$ rectangles with the large silver line centered.

In previous work by Steenari et al. the same type of solar cells had been thoroughly studied. By using the reported silver content of a 0.5 cm^2 silver line containing $3.8 \text{ mg} \pm 0.5 \text{ mg}$ silver, the silver concentration on the $3 \times 5 \text{ cm}^2$ samples was determined [14].

3.3 Vaporisation Test

To find how much leachate vaporises while bubbling air through the solution, 40 ml of 0.5 M nitric acid was put in three 400 ml beakers where two were covered with Parafilm and one was left without. The air flow syringe was then put into the liquid at maximum flow rate (1662 ml/min) and left overnight.

To reduce vaporisation a few drops of surfactant, ethanol, was added to the beakers to reduce bubble size and reduce splashing, in addition to pre-saturating the air flowing into the beakers with water [31].

3.4 Leaching Experiments

A $3 \times 5 \text{ cm}^2$ was put in a 400 ml beaker with leaching solution. The air flow was set to 55.2 ml/min per beaker. A sample was taken every hour during the first 8 h, then every two hours up to 24 and 34 hours. Outside working hours the leaching experiments was paused by dipping the solar cell in mQ-water (Merck Milli-Q Advantage A10). It was then resumed by being re-introduced to the leachate on the next day. Samples were taken by removing 20 μL of leachate at each sampling time. When the experiments were finished the solar cells were dipped in mQ-water, left to dry and saved for future analysis. Acids used and their respective purity and concentration can be found in table 3.1.

Table 3.1: Acids used for leaching, their purity and at what concentrations they were used.

Acid	Empirical Formula	Purity (%)	Concentration (M)	Provider
Citric Acid	$C_6H_8O_7$	≥ 99.5	1, 2	Sigma-Aldrich
Maleic Acid	$C_4H_4O_4$	≥ 99.0	1, 2	Sigma-Aldrich
Nitric Acid	HNO_3	≥ 99.0	0.5, 1.25, 2	Sigma-Aldrich
Oxalic Acid	$C_2H_2O_4$	99.999	1	Sigma-Aldrich

3.5 Sample Analysis

The sample of 20 μL taken from the leachate was diluted in 9.98 mL nitric acid (0.5 M) to get a dilution factor of 500. From the diluted sample 0.5 mL was added to 9.5 mL nitric acid to get a second dilution factor of 10 000. The liquid samples were then analyzed by ICP-MS (Thermo Fisher iCap Q) at an appropriate dilution factor to fit the standard's interval.

The solar cell parts left after leaching were analyzed by SEM and EDX (Thermo Scientific Phenom ProX Desktop SEM) and any solid residue was dried for 24 h in an oven at 50°C . The powder was collected and analyzed by XRD (Bruker D8 Advance).

3.6 Factorial Design

A 2^3 factorial design was conducted based on the results from Steenari et al. [14] and the initial leaching experiments in this work. The acid used was nitric acid and three parameters were investigated; time (1, 4 and 8 h), acid concentration (0.5, 1.25 and 2 M) and solid to liquid ratio (1/20, 1/40 and 1/60 g/ml). Sample data was analysed statistically by ANOVA analysis, regression and three models were constructed from the data. Data response for the models were determined to be silver concentration, silver purity and silver purity by time.

4

Results and Discussion

4.1 Thermodynamic Investigation

Using thermodynamics to find possible leaching routes was the first step prior to real experiments. Dissolution of silver and other elements by nitric, oxalic, citric, maleic, adipic and valeric acid were evaluated accordingly. First the acids were compared to each other in figure 4.1, as can be seen, citric acid has the lowest ΔG° towards silver leaching, however it was also active toward leaching the other metals, see figure 4.2. This is the general trend for all acids, which is not very surprising since silver, being more noble than the other metals, is more difficult to ionize. No acid was found to favor silver only during the thermodynamic investigation.

Leaching of ITO was next to be investigated, the results are presented in figure 4.3 and 4.4. As can be seen, oxalic acid is at a thermodynamic disadvantage to dissolve indium oxide.

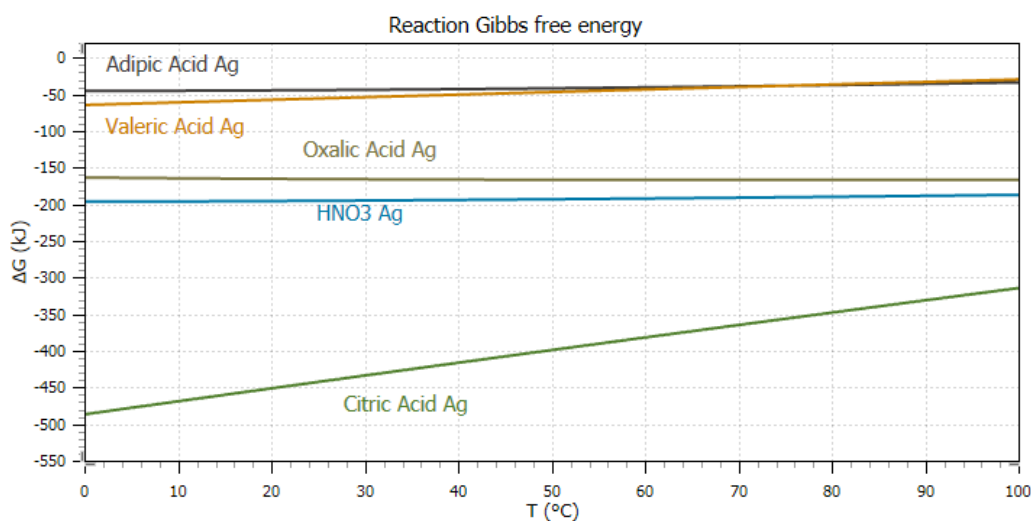


Figure 4.1: ΔG° for the dissolution of silver with different organic acids.

4. Results and Discussion

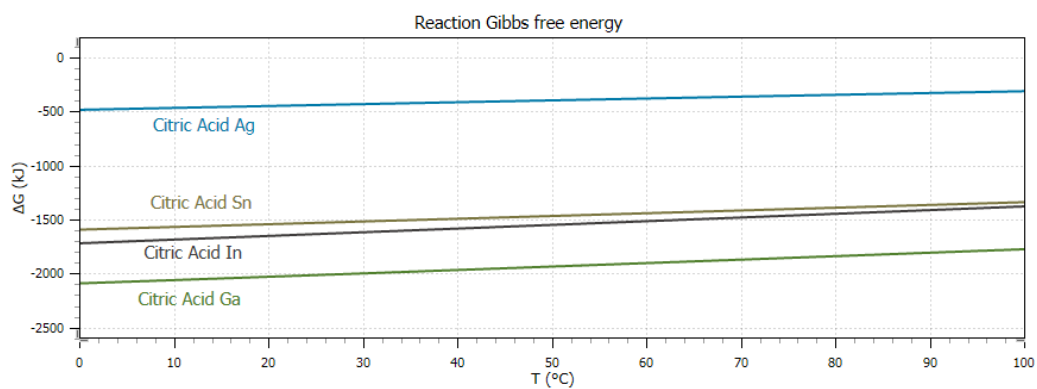


Figure 4.2: ΔG° for reactions with CIGS elements with citric acid.

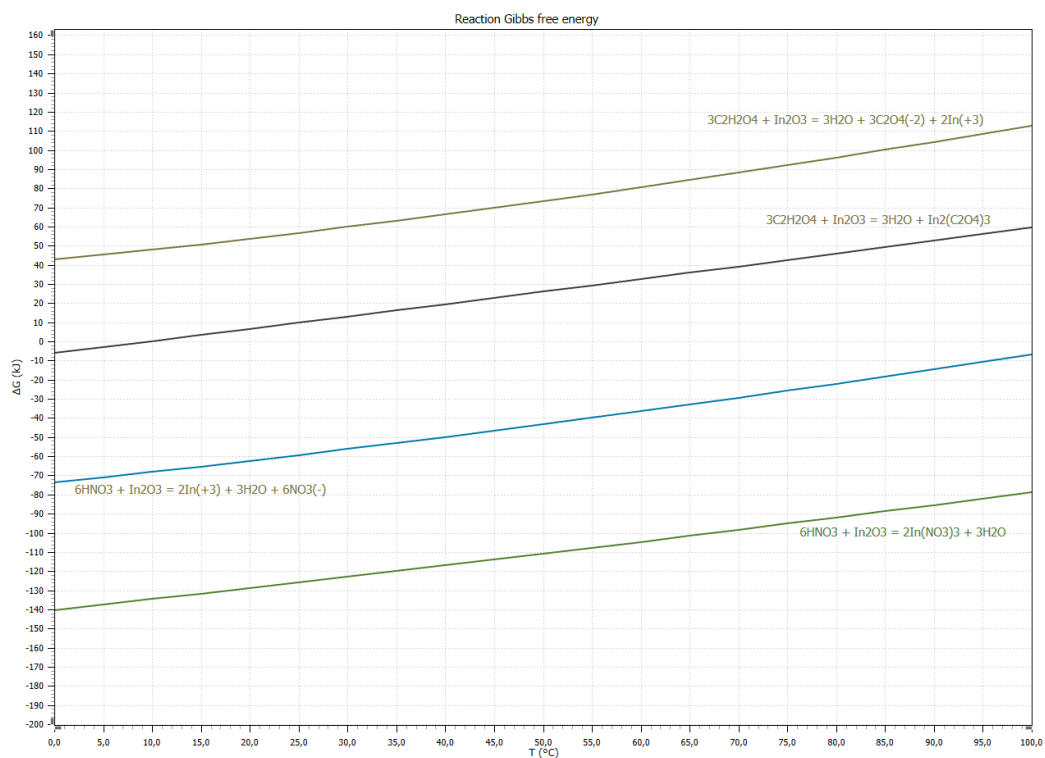


Figure 4.3: ΔG° for ITO reaction with nitric acid and oxalic acid.

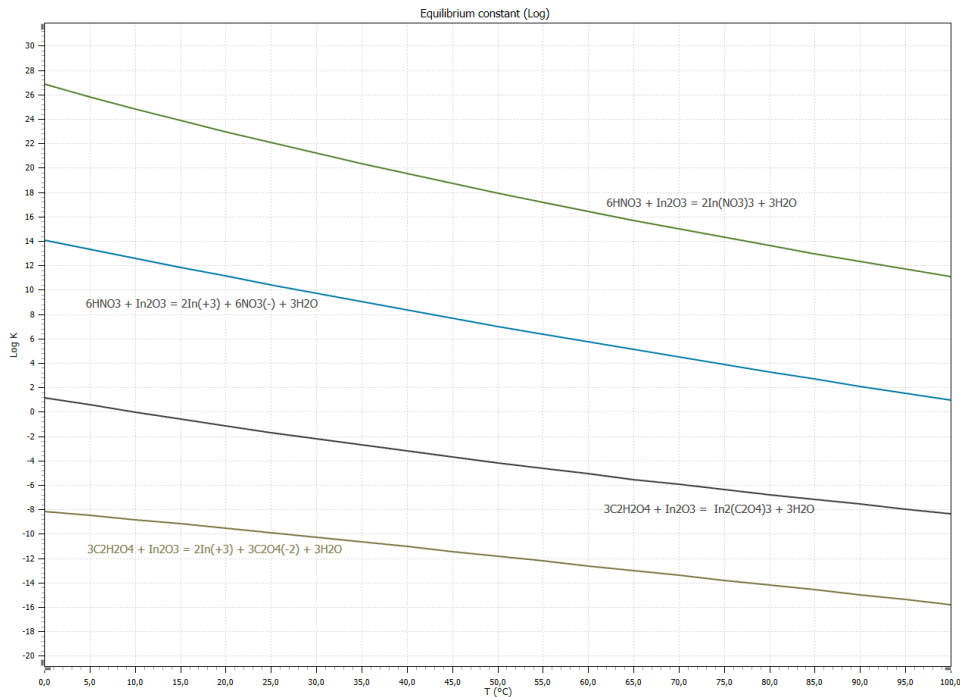


Figure 4.4: Logarithmic value of reaction equilibrium constant for ITO reaction with nitric acid and oxalic acid.

4.2 Vaporization Test

The volume left in the beakers after 24 hours can be seen in table 4.1 below. This investigation indicates that a significant amount of leachate is vaporizing during air bubbling experiments and the liquid loss needs to be taken in consideration. However, without bubbling the leachate volume did not decrease more than 1 mL after 8 hours.

Table 4.1: The volumes before and after 24 hours in the three beakers with and without cover at maximum airflow.

Sample Name	Initial volume (ml)	Final volume (ml)
Open Beaker	40	21
Covered Beaker 1	-"-	32
Covered Beaker 2	-"-	34

The air flow was significantly reduced during the leaching experiments due to this fact and volume loss was taken in consideration when calculating concentrations.

4.3 Initial Leaching Experiments

Initially solar cell samples were leached by 0.5 M nitric acid, 1 and 2 M maleic acid, 1 and 2 M citric acid and 1 M oxalic acid respectively. The samples were leached from 1- to 24h at the room temperature. This was done to investigate the dissolution kinetics of the metals in order to find possible selective leaching strategies.

As can be seen in figure 4.5 the silver concentration in the leachate is around 0 ppm for all samples except nitric acid. Indium and tin can be found in the leachate however, which suggest that the ITO layer is being dissolved. Neither copper, gallium or selenium is found in the leachate which suggest either that the ITO layer was not fully dissolved or that the acids did not favor dissolution of said elements. Observing the dissolution of indium and tin by oxalic acid in figure 4.5 it can be seen, contrary to the thermodynamic investigation in figure 4.3, that oxalic acid efficiently dissolves the ITO layer. This suggest that the acids used probably does not favor the dissolution of copper, gallium and selenium. Since the three elements not found in the dissolution exist only in the CIGS layer, it can be an indication that CIGS remain unaffected at these conditions. Looking at the leaching experiments from a silver leaching perspective however, only nitric acid seems viable as it is the only acid where silver was found in the leachate.

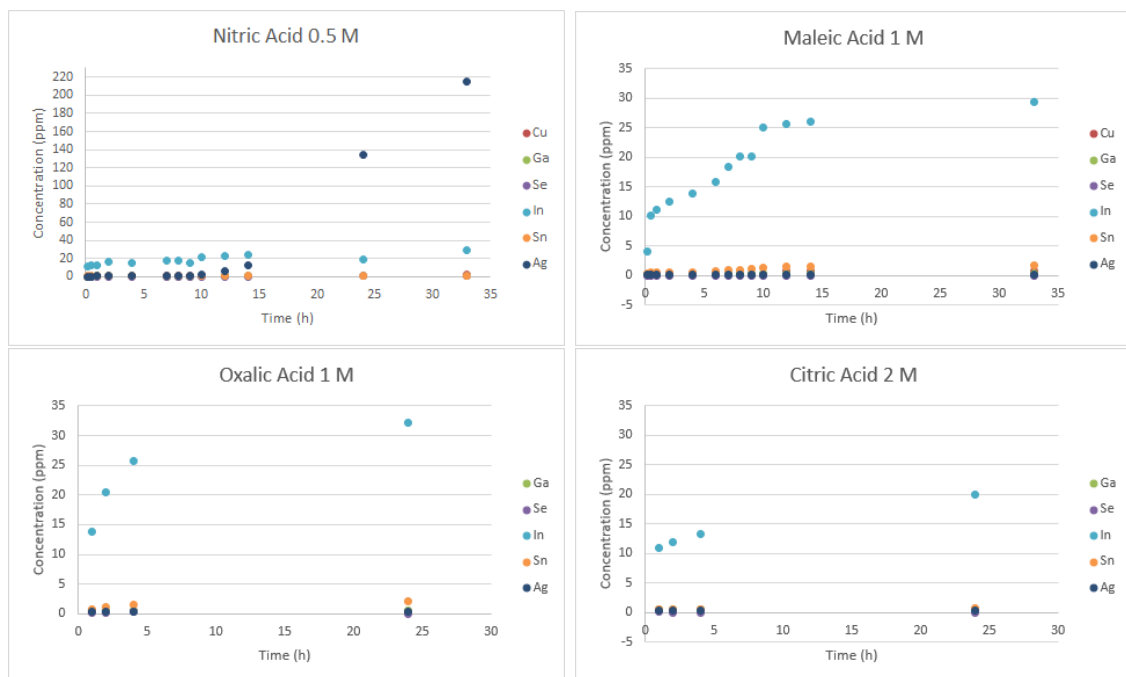


Figure 4.5: Concentrations of metals during leaching with nitric acid, maleic acid, oxalic acid and citric acid.

By observing the solar cell from the oxalic acid, see fig 4.6 it can be seen that a lot of the silver on the cell has been removed when compared to a fresh solar cell, this statement was supported by EDX analysis, see figure 4.7. Further investigation of

the EDX image is that the white part of the image consist mostly of oxygen and molybdenum, this makes the question arise if the black iron oxide particles seeming to stick out of the cell attached to the cell via the leachate or are coming from below the back contact. Further investigation is necessary to understand the iron oxide growth phenomena. More images are included in the appendix, see appendix 2 (B).

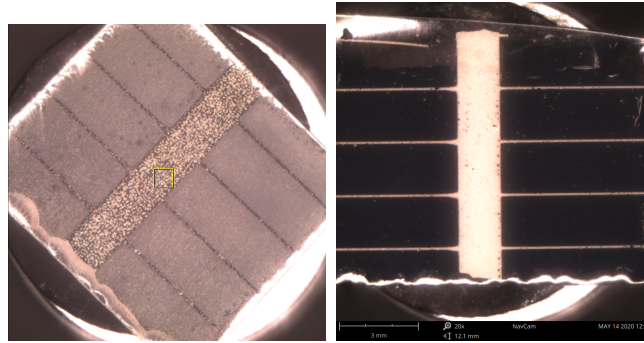


Figure 4.6: SEM images of a sample after 24 h oxalic acid leaching (left) and a fresh sample (right).

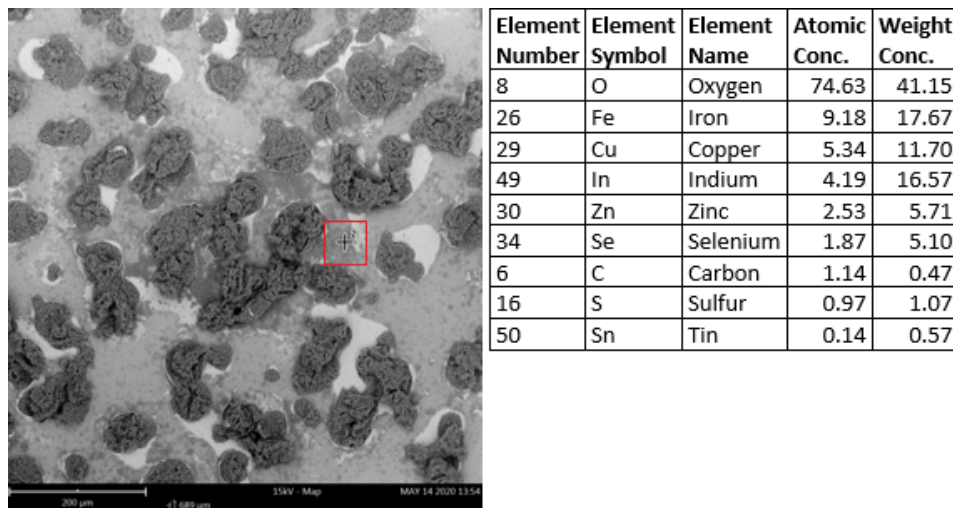


Figure 4.7: EDS analysis on silver conducting line after 24 h oxalic acid leaching.

4. Results and Discussion

There was a pale yellow powder with white lumps residue. Considering that no silver was found in the oxalic acid leachate, it may have precipitated. A possible precipitation route is that a cementation reaction occurred reducing the dissolved silver resulting in metallic silver particles. This might explain the rapid dissolution of indium. After XRD analysis, see fig 4.8 of the powder it was found that the powder's main component was iron oxide followed by oxalic acid dihydrate powder. Since the total silver amount on a sample is approximately 9 mg it is less than 1% of the total mass of the sample (1 g) which is difficult to see in a XRD analysis. The peaks were slightly shifted however, suggesting impurities in the crystal structure, which could potentially be silver. Thus oxalic acid seem to remove silver from the cell efficiently after 24 h of leaching, but it also removes a lot of iron from the substrate. It might be possible to have a one step process where indium is leached simultaneously as silver is precipitated if the amount of co-precipitated iron can be reduced.

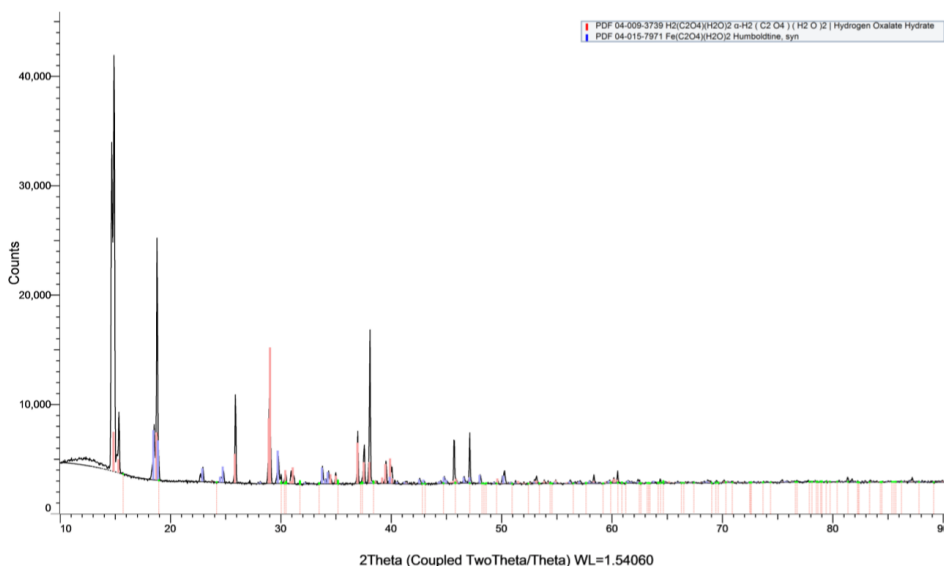


Figure 4.8: XRD spectrum of the residue of the oxalic acid leaching.

4.4 Design of experiments

After the initial leaching experiment a factorial design experiment was conducted to find a model describing silver leached with time, acid concentration and solid to liquid ratio as parameters with variations shown in table 4.2. The parameters time, acid concentration and solid to liquid ratio were chosen to utilize data from the initial leaching experiments and to make this study comparable to previous studies. The factor levels were determined by observing previous studies to investigate an interval where the significance of the parameters were not yet determined and dissolution of silver confirmed [14].

Table 4.2: The design of experiments with result values from Steenari et al. [14] and initial experiments done in this research. The sign table represents the level of the parameter value, a plus sign '+' represents the high value and a minus sign '-' represents the low value of the parameters where A = time, B = Acid concentration and C = S/L ratio. There are two result columns, one for each repetition.

A	B	C	Time (h)	[Acid] (M)	S/L (g/mL)	[Ag] (ppm) 1	[Ag] (ppm) 2
-	-	-	1	0.5	1/60	0.474	0.923
+	-	-	8	0.5	1/60	144.34	139.0
-	+	-	1	2	1/60	111	84
+	+	-	8	2	1/60	98	101
-	-	+	1	0.5	1/20	0.138	0.210
+	-	+	8	0.5	1/20	51.66	43.0
-	+	+	1	2	1/20	67	77
+	+	+	8	2	1/20	412	442

When constructing a model that only consider maximum silver concentration with values from table 4.2 it was realised that only focusing on silver concentration will not yield a method which selectively leaches silver. To find a model that describes selectivity, the silver purity (wt%) was used as response, see table 4.3. The standard deviation of the system, analyzing the center point experiments, is 13 % regarding silver concentration and 3.8 % regarding silver purity with a 95 % confidence interval.

In table 4.3 it can be seen that there are some different conditions that all favor silver purity. By just observing silver purity it is possible to find what conditions are possible candidates to selective leaching within the given interval. However, it should be mentioned that this model is just the first step toward finding the overall optimal conditions for selective leaching. As can be seen in table 4.4 there are three main effects governing the outcome of the model. Take note that factor C, solid to liquid ratio, is not significant. This suggest either that the nitric acid available in solution or silver nitrate saturation at current concentrations are not limiting the kinetics of silver dissolution. This can be tested and confirmed by performing tests with a decreased solid to liquid ratio.

4. Results and Discussion

Table 4.3: The relative silver purity, total silver concentration divided by total metal concentration per sample.

Time (h)	[Acid]	S/L (g/ml)	Ag purity (%) 1	Ag purity (%) 2
1	0.5	1/60	1.75	5.15
8	0.5	1/60	85.6	83.4
1	2	1/60	90.77	85.3
8	2	1/60	89.9	77.1
1	0.5	1/20	0.796	5.67
8	0.5	1/20	82.2	80.9
1	2	1/20	68.2	85.2
8	2	1/20	90.4	88.2

Table 4.4: Effect estimate summary for maximum silver purity. Percent contribution relates to model effect contribution.

Effect estimate summary			
Factor	Effect est	SS	Percent contribution
Time (A)	41.9	7013.0	35.6
[Acid] (B)	41.2	6792.2	34.5
S/L (C)	-2.19	19.1	0.10
AB	-37.8	5721.4	29.0
AC	3.59	51.5	0.26
BC	-0.59	1.40	0.01
ABC	4.97	98.6	0.50

Table 4.5: ANOVA table for silver purity model, a P-value below 0.05 is considered significant.

Source of variation	SS	DF	MS	F0	P-value
Time (A)	7013.1	1	7013.1	212.7	0.00299
Acid Conc (B)	6792.2	1	6792.2	206.0	0.00309
S/L (C)	19.13	1	19.13	0.58	0.66523
AB	5721.4	1	5721.4	173.6	0.00366
AC	51.54	1	51.54	1.56	0.36224
BC	1.40	1	1.40	0.042	0.97308
ABC	98.6	1	98.6	2.99	0.20533
Error	263.7	8	32.96		
Total	19961.1	15			

After the ANOVA analysis was made it was even more clear that S/L ratio was not significant as the P-value suggest. This is probably due to the leachate not being close to saturation at these conditions. As can be seen in the response surface of the mode, figure 4.9, there are more than one outcome with high silver purity. It does however not reflect the amount of silver in the solution, for example; the

silver purity for one hour of leaching in 2M nitric acid are close to the purity of the same concentration after 8 hours. The concentrations at these two times are: 111 and 412 ppm respectively, the correlation between silver concentration, purity and time are not linear. This suggest that leaching for one hour could lead to a higher total concentration if fresh samples were to be used after one hour with the same leachate. It should be mentioned that as long as the acid is consumed by the leaching process it can be expected that the kinetics will change over time. This can be investigated by measuring pH. The saturation of the leachate is also a parameter that will reduce leaching rate over time. A secondary issue with this method is that the cells still contain silver after 1 h of leaching, to recover all of the silver it might be possible to add a second leaching step. The second step however, will need different conditions to reach high silver purity as it has previously been seen that increased time may decrease silver purity, see fig 4.9. It might be possible to change the leaching conditions in the second solution to a lower nitric acid concentration which has proven to favor high silver purity even after 8 h.

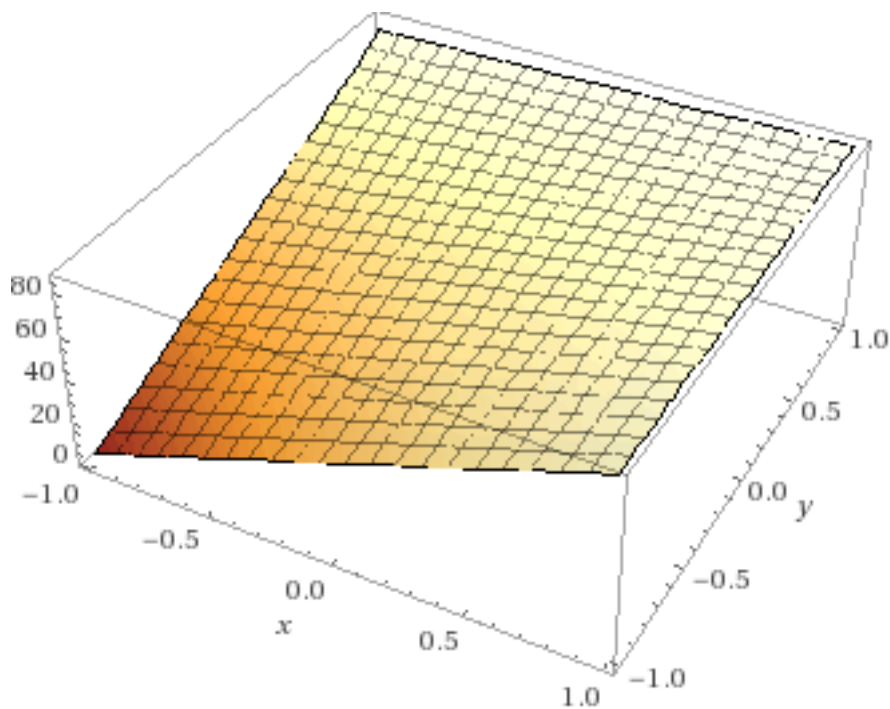


Figure 4.9: Response surface for silver purity model as a function of time (x) vs acid concentration (y) with silver purity % response (z). Brighter color is higher purity.

By changing the response to silver purity divided by time, see figure 4.10, it can be seen what conditions favor the highest purity in the least amount of time. This makes it easier to see the non-linear relation between time and purity. The response surface suggest that going for short leaching time and high concentration yield the highest purity. This may be an indication of silver being the kinetic product of the system and that as time progress the other metals start dissolving more rapidly.

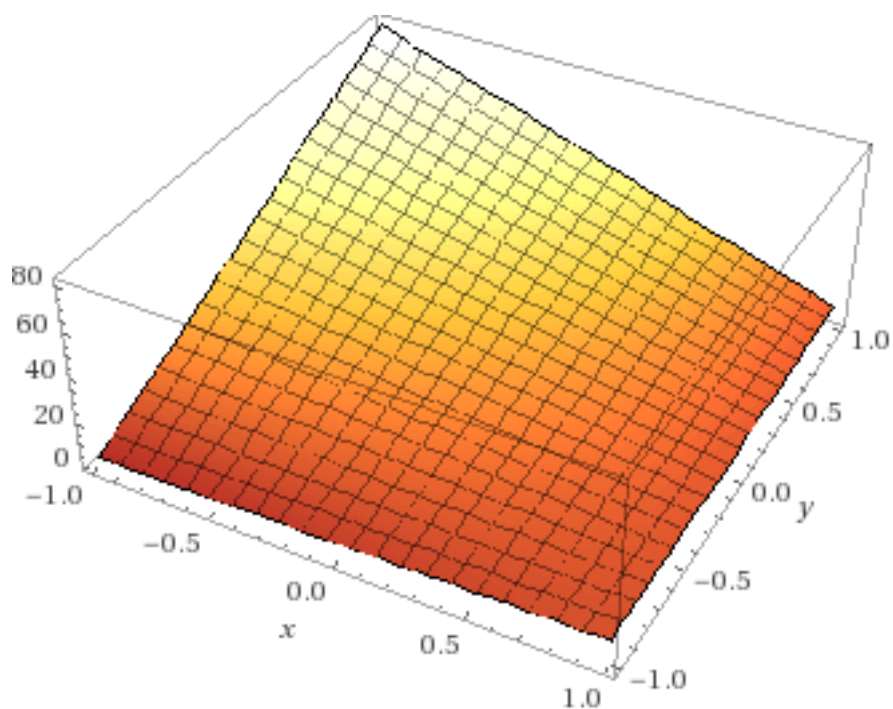


Figure 4.10: The response surface for silver purity divided by time, take note that it has the same shape as figure 4.9 but inverted. X represents time, Y represents acid concentration and Z is the purity divided by time.

5

Conclusions

This study investigated silver dissolution by selective leaching from CIGS solar cells. Silver recovery is an important step toward a sustainable solar panel market by recycling of spent solar cells. It is an initial step toward obtaining an efficient and selective silver leaching system with nitric acid. By investigating silver dissolution by different organic acids and nitric acid followed by a factorial design it was possible to find that an interaction between time and acid concentration is affecting the silver purity whereas solid to liquid ratio was found to not affect the resulting purity and silver concentration at the examined interval. While providing valuable hints on what is the next step in further research, using factorial design saved a lot of time making it possible to conclude this study on time. The significant factors are time and nitric acid concentration within the interval 1-8 h, 0.5-2 M acid concentration and 1/20-1/60 g/mL solid to liquid ratio where the resulting silver purity was 90 % after 1 h leaching. A solid residue found after 24 h leaching by oxalic acid. It's main components were iron oxalate and oxalic acid hydrate. The possible cementation reaction can become a potential step in CIGS recycling by providing a leaching step which separates both silver and indium from the cell simultaneously.

References

- [1] *Energy - United Nations Sustainable Development*. URL: <https://www.un.org/sustainabledevelopment/energy/>.
- [2] A Jäger-Waldau. “PV Status Report 2019, EUR 29938 EN”. In: *Publications Office of the European Union, Luxembourg* (2019).
- [3] IRENA. *Renewable Energy Statistics 2019*. Abu Dhabi: The International Renewable Energy Agency, 2019.
- [4] Adam Rose. “China’s solar capacity overtakes Germany in 2015, industry data show”. In: *Reuters* (Jan. 2016). URL: <https://www.reuters.com/article/china-solar-idUSL3N15533U>.
- [5] Stephanie Weckend IRENA, Andreas Wade IEA-PVPPF, and Gavin Heath IEA-PVPPF. *End-of-life management Solar Photovoltaic Panels*. Jan. 2016. URL: <https://www.irena.org/publications/2016/Jun/End-of-life-management-Solar-Photovoltaic-Panels>.
- [6] Jeyakumar Ramanujam et al. “Inorganic photovoltaics – Planar and nanostructured devices”. In: *Progress in Materials Science* 82 (2016), pp. 294–404. ISSN: 0079-6425. DOI: <https://doi.org/10.1016/j.pmatsci.2016.03.005>. URL: <http://www.sciencedirect.com/science/article/pii/S0079642516300056>.
- [7] Harry Hahn et al. “Untersuchungen über ternäre Chalkogenide. V. Über einige ternäre Chalkogenide mit Chalkopyritstruktur”. In: *Zeitschrift für anorganische und allgemeine Chemie* 271.3-4 (1953), pp. 153–170. DOI: 10.1002/zaac.19532710307. eprint: <https://onlinelibrary.wiley.com/doi/pdf/10.1002/zaac.19532710307>. URL: <https://onlinelibrary.wiley.com/doi/abs/10.1002/zaac.19532710307>.
- [8] Angus MacKinnon. “Ternary semiconductors”. In: *Festkörperprobleme 21: Plenary Lectures of the Divisions “Semiconductor Physics” “Metal Physics” “Low Temperature Physics” “Thermodynamics and Statistical Physics” “Thin Films” “Magnetism” “Quantum Optics” of the German Physical Society Münster, March 9–14, 1981*. Ed. by J. Treusch. Berlin, Heidelberg: Springer Berlin Heidelberg, 1981, pp. 149–165. ISBN: 978-3-540-75368-1. DOI: 10.1007/BFb0108603. URL: <https://doi.org/10.1007/BFb0108603>.
- [9] Yi-Chih Wang and Han-Ping D. Shieh. “Double-graded bandgap in Cu(In,Ga)Se₂ thin film solar cells by low toxicity selenization process”. In: *Applied Physics Letters* 105.7 (2014), p. 073901. DOI: 10.1063/1.4893713. eprint: <https://doi.org/10.1063/1.4893713>. URL: <https://doi.org/10.1063/1.4893713>.

- [10] Jeyakumar Ramanujam and Udai P. Singh. “Copper indium gallium selenide based solar cells – a review”. In: *Energy & Environmental Science* 10.6 (Apr. 2017), pp. 1306–1319. DOI: 10.1039/c7ee00826k.
- [11] Eduardo Ribeiro et al. “CdS versus ZnSnO buffer layers for a CIGS solar cell: A depth-resolved analysis using the muon probe”. In: *EPJ Web of Conferences*. Vol. 233. EDP Sciences. 2020, p. 05004.
- [12] K. L. Chopra, P. D. Paulson, and V. Dutta. “Thin-film solar cells: an overview”. In: *Progress in Photovoltaics: Research and Applications* 12.2-3 (2004), pp. 69–92. DOI: 10.1002/pip.541. eprint: <https://onlinelibrary.wiley.com/doi/pdf/10.1002/pip.541>. URL: <https://onlinelibrary.wiley.com/doi/abs/10.1002/pip.541>.
- [13] Leena Grandell and Andrea Thorenz. “Silver supply risk analysis for the solar sector”. In: *Renewable Energy* 69 (2014), pp. 157–165. ISSN: 0960-1481. DOI: <https://doi.org/10.1016/j.renene.2014.03.032>. URL: <http://www.sciencedirect.com/science/article/pii/S0960148114001785>.
- [14] Britt-Marie Steenari, Burcak Ebin, and Lovisa Baun. *Recycling of silver from CIGS solar cells*. 2018, pp. 1–26.
- [15] M.Salim Öncel, Mahir Ince, and Mahmut Bayramoglu. “Leaching of silver from solid waste using ultrasound assisted thiourea method”. In: *Ultrasonics Sonochemistry* 12.3 (2005), pp. 237–242. ISSN: 1350-4177. DOI: <https://doi.org/10.1016/j.ultsonch.2003.10.007>. URL: <http://www.sciencedirect.com/science/article/pii/S1350417703002037>.
- [16] Harnchana Gatemala, Sanong Ekgasit, and Kanet Wongravee. “High purity silver microcrystals recovered from silver wastes by eco-friendly process using hydrogen peroxide”. In: *Chemosphere* 178 (2017), pp. 249–258. ISSN: 0045-6535. DOI: <https://doi.org/10.1016/j.chemosphere.2017.03.051>. URL: <http://www.sciencedirect.com/science/article/pii/S0045653517304149>.
- [17] Wojciech Hyk and Konrad Kitka. “Highly efficient and selective leaching of silver from electronic scrap in the base-activated persulfate - ammonia system”. In: *Waste management (New York, N.Y.)* 60 (Jan. 2017). DOI: 10.1016/j.wasman.2016.12.038.
- [18] Simon Philipps and Werner Warmuth. “Photovoltaics report—Fraunhofer ISE”. In: *Fraunhofer Institute for Solar Energy Systems ISE*. url: <http://www.ise.fraunhofer.de/en/publications/studies/photovoltaics-report.html> (visited on 06/03/2020) (2018).
- [19] Ananya Baksi et al. “Extraction of Silver by Glucose”. In: *Angewandte Chemie International Edition* 55.27 (2016), pp. 7777–7781. DOI: 10.1002/anie.201510122. eprint: <https://onlinelibrary.wiley.com/doi/pdf/10.1002/anie.201510122>. URL: <https://onlinelibrary.wiley.com/doi/abs/10.1002/anie.201510122>.
- [20] Harnchana Gatemala, Sanong Ekgasit, and Kanet Wongravee. “High purity silver microcrystals recovered from silver wastes by eco-friendly process using hydrogen peroxide”. In: *Chemosphere* 178 (2017), pp. 249–258. ISSN: 0045-6535. DOI: <https://doi.org/10.1016/j.chemosphere.2017.03.051>. URL: <http://www.sciencedirect.com/science/article/pii/S0045653517304149>.

-
- [21] Pierre Perrot. *A to Z of Thermodynamics*. Oxford University Press on Demand, 1998.
- [22] Krister Ström. *Grundläggande separationsteknik*. 4. uppl. Göteborg: Chalmers tekn. högsk., Inst. för kemisk apparat- & anläggningsteknik, 1999.
- [23] Douglas Montgomery. *Design and Analysis of Experiments*. John Wiley & Sons, Inc., 2013, pp. 1–21. ISBN: 978-1-118-09793-9.
- [24] Douglas Montgomery. *Design and Analysis of Experiments*. John Wiley & Sons, Inc., 2013, pp. 554–569. ISBN: 978-1-118-09793-9.
- [25] Douglas Montgomery. *Design and Analysis of Experiments*. John Wiley & Sons, Inc., 2013, pp. 241–253. ISBN: 978-1-118-09793-9.
- [26] Fadi R. Abou-Shakra. “Chapter 12 - Biomedical applications of inductively coupled plasma mass spectrometry (ICP–MS) as an element specific detector for chromatographic separations”. In: *Bioanalytical Separations*. Ed. by Ian D. Wilson. Vol. 4. Handbook of Analytical Separations. Elsevier Science B.V., 2003, pp. 351–371. DOI: [https://doi.org/10.1016/S1567-7192\(03\)80013-X](https://doi.org/10.1016/S1567-7192(03)80013-X). URL: <http://www.sciencedirect.com/science/article/pii/S156771920380013X>.
- [27] A Mark Pollard et al. *Analytical chemistry in archaeology*. Cambridge University Press, 2007.
- [28] Simon Maher, Fred PM Jjunju, and Stephen Taylor. “Colloquium: 100 years of mass spectrometry: Perspectives and future trends”. In: *Reviews of Modern Physics* 87.1 (2015), p. 113.
- [29] Joseph I Goldstein et al. *Scanning electron microscopy and X-ray microanalysis*. Springer, 2017, pp. 21–60.
- [30] Joseph I Goldstein et al. *Scanning electron microscopy and X-ray microanalysis*. Springer, 2017, pp. 297–353.
- [31] Maedeh Asari and Faramarz Hormozi. “Effects of Surfactant on Bubble Size Distribution and Gas Hold-up in a Bubble Column”. In: *American Journal of Chemical Engineering* 1.2 (2013), pp. 50–58. DOI: 10.11648/j.ajche.20130102.14. URL: <http://www.sciencepublishinggroup.com/journal/paperinfo.aspx?journalid=224&doi=10.11648/j.ajche.20130102.14>.

A

Appendix 1 - Design of Experiments Data

Effect estimate summary			
Factor	Effect est	SS	Percent contribution
A	136.2876	74297.25	28.32903
B	126.5262	64035.54	24.41631
C	51.78615	10727.22	4.090215
AB	42.21239	7127.544	2.717683
AC	64.79832	16795.29	6.403928
BC	99.21385	39373.55	15.01286
ABC	111.7017	49909.06	19.02998

Table A.1: Summary of effects when optimizing towards maximum silver concentration.

ANOVA table				
Source of variation	Sum sq	DF	Mean sq	F ₀
Time (A)	4163.161	1	4163.161	187.299
Acid Conc (B)	6312.445	1	6312.445	283.9945
S/L (C)	25.09417	1	25.09417	1.128977
AB	6178.592	1	6178.592	277.9725
AC	37.24912	1	37.24912	1.675824
BC	31.37394	1	31.37394	1.411502
ABC	35.42521	1	35.42521	1.593767
Error	177.8188	8	22.22735	
Total	16961.16	15		

Table A.2: ANOVA table for maximum silver concentration after investigating each leaching parameter in the factorial experiment.

$$y = \beta_0 + \frac{1}{2}(\beta_1x_1 + \beta_2x_2 + \beta_{23}x_2x_3 + \beta_{123}x_1x_2x_3) \quad (\text{A.1})$$

β_0	110.74
β_1	136.29
β_2	126.53
β_{23}	99.21
β_{123}	111.70
R^2	0.865

Table A.3: predicted model for maximum silver concentration.

ANOVA table

Source of variation	Sum sq	DF	Mean sq	F0
Time (A)	4163,161	1	4163,161	187,299
Acid Conc (B)	6312,445	1	6312,445	283,9945
S/L (C)	25,09417	1	25,09417	1,128977
AB	6178,592	1	6178,592	277,9725
AC	37,24912	1	37,24912	1,675824
BC	31,37394	1	31,37394	1,411502
ABC	35,42521	1	35,42521	1,593767
Error	177,8188	8	22,22735	
Total	16961,16	15		

Table A.4: ANOVA table for Silver purity per hour.

B

Appendix 2 - SEM and EDS images

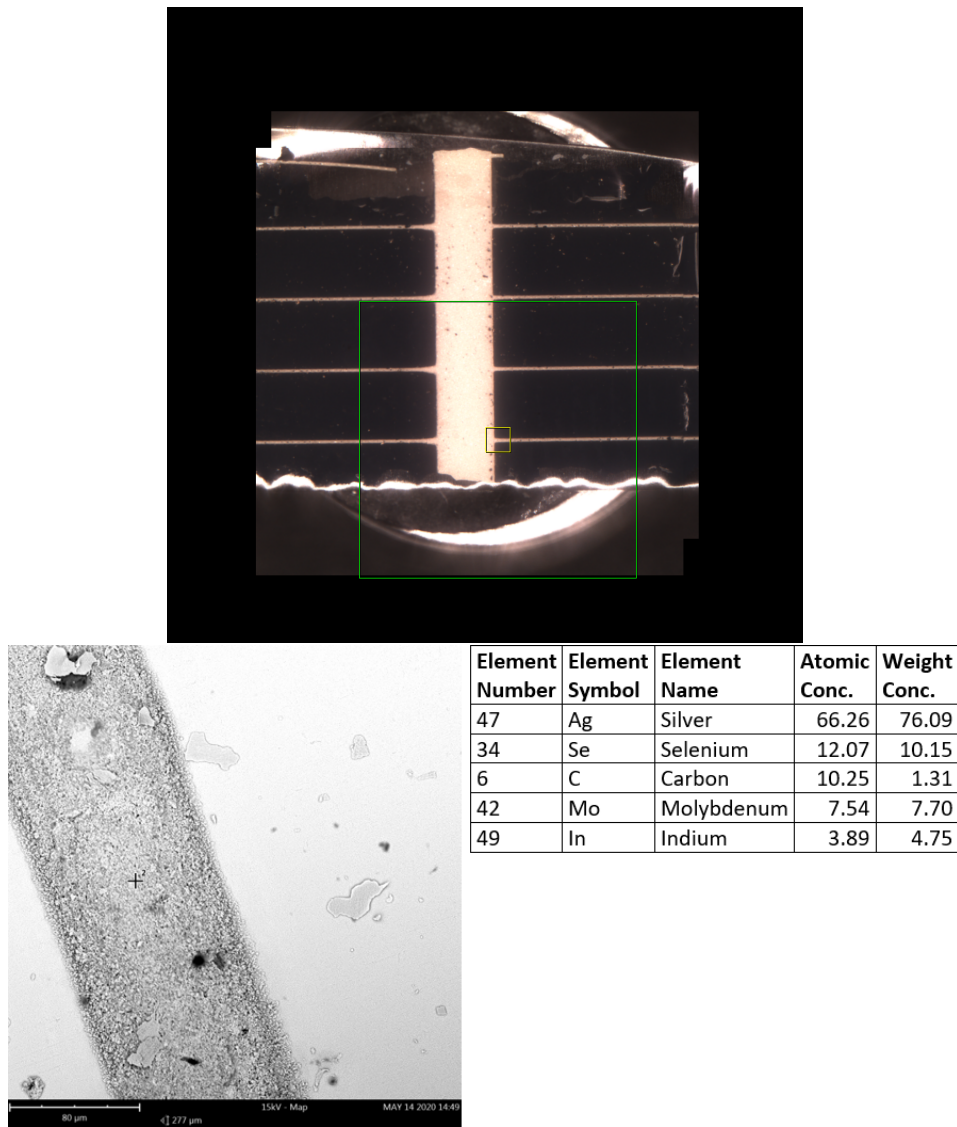


Figure B.1: Analysis of fresh solar cell showing original composition of silver line.

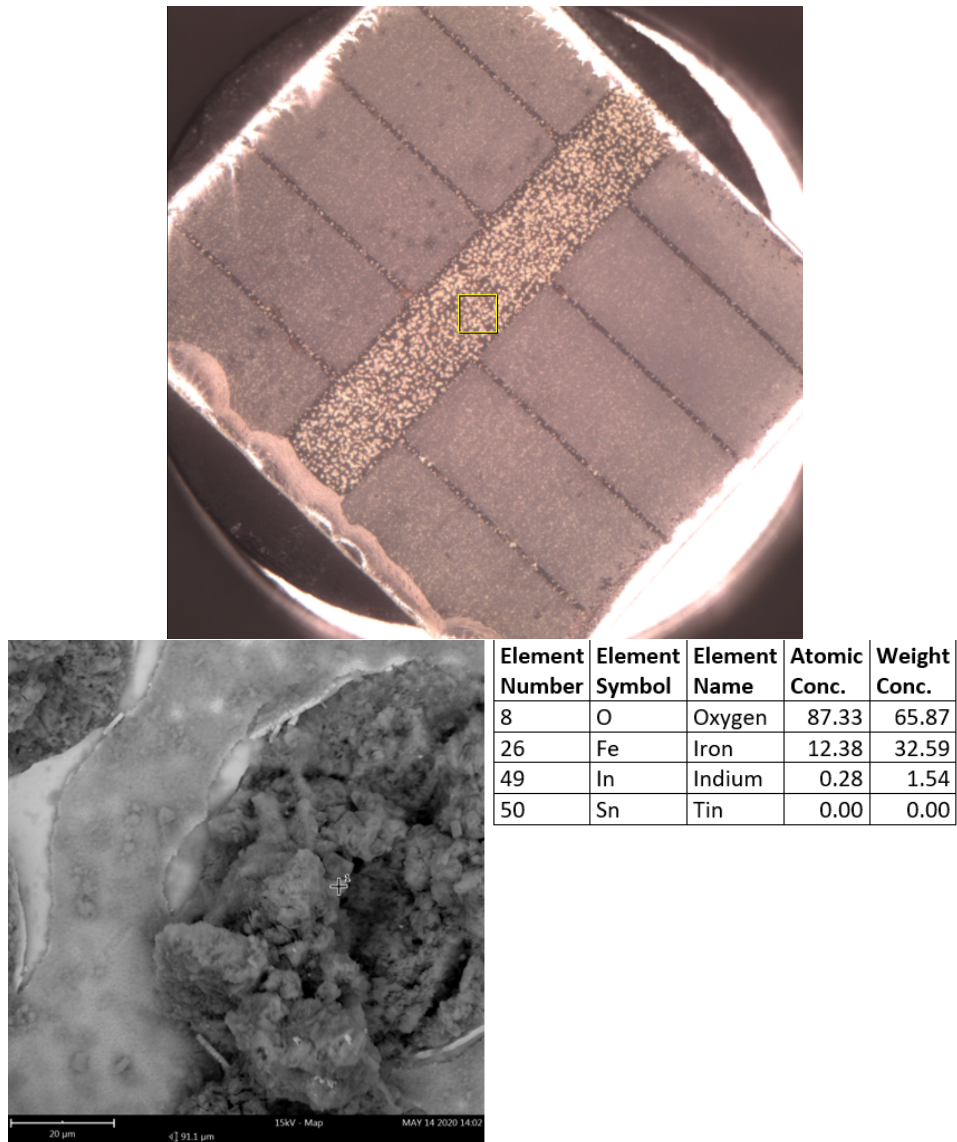


Figure B.2: Analysis of cell after 24h of oxalic acid leaching on silver line. No Silver present. Bottom image is EDX of the black lump.

C

Supplementary Data

Nitric Acid

When arriving the day after the sample was put in nitric acid the air had stopped bubbling, it is not known when the bubbles stopped. The last sample was therefore taken at the 24 h mark and not left in there for longer. This led to some changes in the air setup.

0.5 M Observations

Right after the solar cell sample was put in nitric acid it look as if a small layer of the sample started to peel off toward the silver lines. It ended up as small white particles on the bottom of the beaker. After 24 hours the layer had still not disappeared completely, about a quarter of the sample was still covered.

The silver lines faded slowly with time from a bright white into a brown, yellow-ish tint. The silver lines was still not completely gone after 24 hours.

Oxalic Acid

1 M Observations

After 4 hours the solar cell had start to turn purple, after 6 hours the liquid was purple as well. After 24 hours it looked like most of the silver had been dissolved or reacted. In addition to the purple liquid there was a solid residue on the bottom of the beaker, after drying it it looked like a yellow solid with white lumps in it

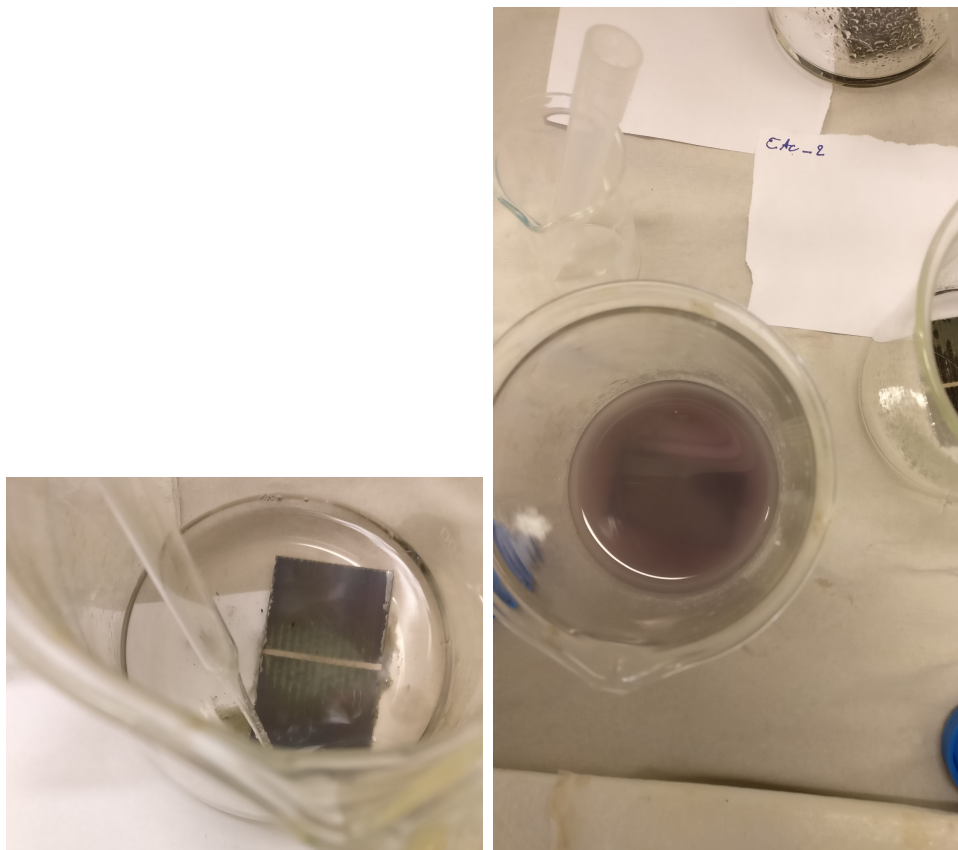


Figure C.1: An image taken above the beaker of the oxalic acid leaching sample after 4 h and 24 h respectively. Notice the slight purple tint of the otherwise green cell and that the leachate had turned purple after 24 h.

Maleic Acid

Observations

When 1 M maleic acid was used and repeated the second repetition had a lot of particles in it after 7 hours.